INTERNATIONAL JOURNAL OF REFRIGERATION 70 (2016) 225–234

Available online at www.sciencedirect.com

ScienceDirect

journal homepage: www.elsevier.com/locate/ijrefrig

Illustrating the relationship between the coefficient of performance and the coefficient of system performance by means of an R404 supermarket refrigeration system

M.R. Braun [a,*], P. Walton [b], S.B.M. Beck [c]

[a] Department of Mechanical Engineering, University of Sheffield, Sheffield, UK
[b] Marks & Spencer, London W2 1AS, UK
[c] Multidisciplinary Engineering Education, University of Sheffield, Sheffield, UK

ARTICLE INFO

Article history:
Received 21 July 2015
Received in revised form 19 October 2015
Accepted 21 October 2015
Available online 30 October 2015

Keywords:
COP
Coefficient of system performance
Supermarket refrigeration system
Condenser fan
System control

ABSTRACT

Because the coefficient of performance (*COP*) is primarily concerned with the core refrigeration system, using it for optimisation purposes may lead to higher than necessary energy consumption. This hypothesis was studied with a simple equation relating this coefficient to the coefficient of system performance (*COSP*), and with a software model based on an R404A refrigeration system installed in a supermarket in north east England. In both approaches the condenser fan power usage was excluded from the *COP* but included in the *COSP*. The results showed that, especially for part load conditions, optimising the core refrigeration system for minimum power consumption led to an appreciably higher overall energy consumption with the implication that the condenser fan and compressor controls should be developed together. When using this holistic approach it was found that energy savings of 4.5% could have been achieved based on six months' data from the installed system.

Illustration de la relation entre le coefficient de performance et le coefficient de performance du système grâce à un système frigorifique de supermarché au R404

Mots clés : COP ; Coefficient de performance du système ; Système frigorifique de supermarché ; Ventilateur de condenseur ; Régulation de système

* Corresponding author. Department of Mechanical Engineering, University of Sheffield, Mappin Street, Sheffield, S. Yorkshire S88AP, UK. Tel.: +4401143275248.
E-mail address: dtp11mrb@sheffield.ac.uk (M.R. Braun).

http://dx.doi.org/10.1016/j.ijrefrig.2015.10.020

Nomenclature

$p_{c,abs}$	absolute condenser pressure
$\dot{V}_{air}$	air mass flow rate
$\bar{c}_p$	average of specific capacity of refrigerant in a vapour region
$\dot{Q}_e$	cooling loads
h_3'	enthalpy at start of condensing process
$\dot{Q}_{cdg}$	heat rejected through condensing part of condenser
$\dot{Q}_{dsh}$	heat rejected through de-superheating part of condenser
$\dot{Q}_c$	heat rejection rate of condenser
$\dot{Q}_{air}$	heat rejection rate to air through condenser
$\dot{m}_{air,cdg}$	mass flow rate of air through condensing part of condenser
$\dot{m}_{air,dsh}$	mass flow rate of air through de-superheating part of condenser
$\dot{m}_{air,max}$	maximum air mass flow rate
n_{mx}	maximum fan speed
$\dot{Q}_{e,max}$	maximum refrigeration effect
E_{cmp}	power input into compressor (including ancillary equipment)
E_{fan}	power input into condenser fan
E_{other}	power input into devices other than compressors and condenser fans
E'_{cmp}	power output of compressor
$\dot{m}_{air,rq}$	required air flow rate
$\dot{m}_{rf}$	required refrigerant mass flow rate
c_{air}	specific heat capacity of air
$\dot{q}_{HX}$	specific heat transferred in heat exchanger
$n_{fn\%}$	speed of condenser fan in % of maximum fan speed
E_{tot}	total power input
$\vec{p}_c$	vector of condenser pressure
$\vec{\dot{Q}}_e$	vector of cooling loads
COP	coefficient of performance
$COSP$	coefficient of system performance
h_1	enthalpy at exit port of evaporator
h_2	enthalpy at entry port of compressor
h_3	enthalpy at exit port of compressor
h_4	enthalpy at exit of condenser
h_5	enthalpy at exit port of high pressure side of heat exchanger
k, j, i	indices
p_c	condenser pressure (general); absolute pressure at discharge port of compressor
p_e	evaporation pressure (general); absolute pressure at suction port of compressor
r^2	coefficient of determination

Greek letters

$\bar{\vartheta}_2$	mean temperature of de-superheating section of the condenser
ϑ_{sh}	superheat temperature
$\vartheta_{l,sat}$	temperature of saturated liquid
$\vartheta_{g,sat}$	temperature of saturated vapour
$\vec{\vartheta}_{on}$	vector of air temperature entering the condenser
ε	effectiveness

1. Introduction

A common way of referring to the efficiency of a cooling application is to quote its coefficient of performance (*COP*). It may be described as the textbook method of calculating the efficiency figure for refrigeration, because textbooks, such as the one authored by Çengel and Boles (2007), use it and define it as the "desired output" over the "required input". This definition, however, is somewhat vague especially as it leaves the term "required input" open to interpretation. The textbook by Arora (2010) seems to offer a stricter definition since it uses the phrase "net energy supplied from external sources", but in ASHRAE handbooks, which also use the exact same wording (ASHRAE, 1997), three different ways are used to define this net energy. One way is for the analysis of a theoretical single-stage cycle where ASHRAE (1997) equates the net supplied energy to the mass of the refrigerant multiplied by its enthalpy change. As this does not take any compressor or motor losses into account, *HVAC Systems and Equipment* (ASHRAE, 2002) substitutes the energy input with the electrical power supplied to the motor terminals (for hermetic or semi-hermetic compressors) or the mechanical power acting on the compressor shaft (for open compressors). Other ways of defining this power or energy input are given in BS EN 13771-1:2003 for compressors and in BS EN 13771-2:2007 for different types of condensing unit.

As the discussion above shows the term "*COP*" can be ambiguous since the supplied energy or power depends on the system boundaries. A different term which more clearly acknowledges this is the term coefficient of system performance (*COSP*). According to da Cunha (2010) this efficiency figure is more frequently used than *COP* as it also includes ancillary loads such as condenser fans and pumps. Other, more practical texts also prefer the term *COSP* over *COP* for the same reason (Pearson, 2008). Different areas of cooling applications employ their own way of characterising the effectiveness of this type of application with comparable problems. One example is the criticism that the power usage effectiveness (PUE) for data centres, which also includes cooling, has attracted. Similarly to the *COP*, one of these criticisms is that it is not clear what is included and what is not as "required inputs" to compute the PUE (Yuventi and Mehdizadeh, 2013).

The potential importance of including the condenser fans can also be seen when considering related fields of research. One example is the work by Manske et al. (2001) who studied an industrial refrigeration system with an evaporative condenser and captured the interplay between the compressor and condenser fan power consumption very well by pointing out that there is a trade-off between the energy used by the compressor and the energy consumption of the fans; which leads to an optimisation problem. Their investigation finds that for a system with minimum overall energy use there is a strong,

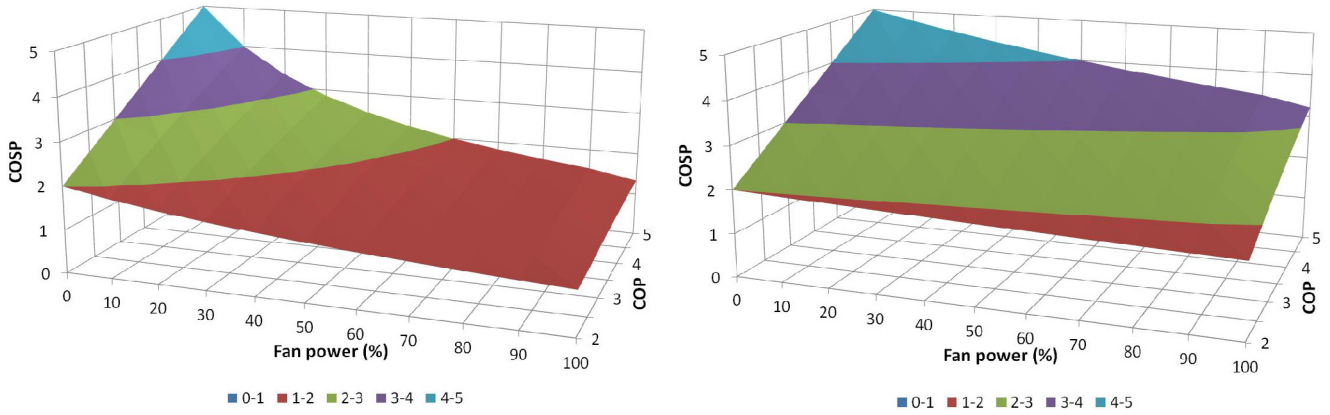

Cooling load = 20% of maximum

Cooling load = 100% of maximum

Fig. 1 – The influence of fan power consumption and COP on COSP.

almost linear relationship between the outdoor wet-bulb temperature and the condenser pressure, but virtually no relationship with the cooling load. Yu and Chan have investigated the same interaction between the compressor power consumption and fan input power of a dry air condenser for chillers and have published extensively in this area. Their findings for various systems with dry condensers (Yu and Chan, 2005; Yu et al., 2006; Yu and Chan, 2008) differ from those by Manske et al. (2001) for an evaporative one. Yu and Chan's results indicate that overall energy consumption depends not only on the outdoor temperature, but also on the cooling load. Both strands of research suggest that the conclusion "fan power is only a small fraction of the total power consumption" (Ge and Tassou, 2000) for supermarket refrigeration systems may not be correct with the implication that fan control algorithms deserve more attention.

Having highlighted the necessity to fully understand a system's boundary and the interplay between system components, this paper aims to show the relationship between the *COP*, which is used here to refer to the core refrigeration system only, and the *COSP*, which includes also ancillary equipment. This is done not only in a theoretical way, but also by using the example of a Matlab model, which is based on an installed system, to illustrate the real energy saving potential of this semantic debate. In that way this paper expands work presented by Braun et al. (2014).

1.1. *Relationship between* COP *and* COSP

As a first step in establishing a relationship between the *COP* for the core refrigeration system and *COSP* for the complete refrigeration system the definition of the *COSP* by Pearson (2008) is written in mathematical form as in Equation (1).

$$COSP = \frac{\dot{Q}_e}{E_{tot}} = \frac{\dot{Q}_e}{E_{cmp} + E_{fan} + E_{other}} \tag{1}$$

If it can be assumed that E_{other} is much smaller than both compressor power E_{cmp} and condenser fan power E_{fan}, it can be neglected. In addition, if the compressor is semi-hermetic (as in the installed system used as the basis for the software model below) then the *COP* equals $\dot{Q}_e/E_{cmp}$ (ASHRAE, 2008). Modifying Equation (1) according to these assumptions yields Equation (2).

$$COSP \cong \frac{COP}{1 + COP\dfrac{E_{fan}}{\dot{Q}_e}} \tag{2}$$

When analysing Equation (2) it is apparent that, when the fan is switched off, the *COP* is equal to the *COSP*. A less obvious result is that when $\dot{Q}_e$ (the cooling load) increases, the relative importance of the power use of the condenser fans diminishes. On the other hand, as the *COP* increases, so does the influence of fan power consumption. Fig. 1 visualises the results of this equation for one part load point ($\dot{Q}_e = 20\%\,\dot{Q}_{e,max}$) and for full load (the maximum fan power is assumed to be 10% of $\dot{Q}_{e,max}$). The graphs in Fig. 1 show that the *COSP* is influenced by the condenser fan, particularly under part-load conditions.

2. Installed R404 supermarket refrigeration system

Two cascaded R404A/CO_2 refrigeration systems installed in a supermarket in the north-east of England with nominal cooling capacities of 60 and 80 kW (Searle Manufacturing Company, 2008) were studied for the software model described in Section 3. Although eventually the larger of the two refrigeration plants was selected, data for both systems were downloaded for the period 1 June 2014 to 30 November 2014 (and prepared in 15 min intervals) and used for intercomparison to detect errors in data acquisition and preparation. The reason for choosing the larger system was that the electricity consumption of the condenser fans could be studied more effectively as there were twice as many fans in the larger system.

The main components of the 80 kW system are arranged similarly to the left hand panel in Fig. 2 and are listed in Table 1. One of the major differences between this figure and the installed system is that the installed system drives the refrigeration system with four reciprocal, semi-hermetic, 4-cylinder individual compressors, which are all controlled from the same controller. Originally, only compressors C1–C3 were fitted. C4 was added later (but before this analysis started) to boost the system's

Table 1 – Main components of the installed refrigeration system.

Component	Model	Qty	Remarks
Refrigerant	R404A	1	
Compressor – C1	Bitzer, 4DC-5.2Y	1	VSD: 20 Hz–60 Hz
Compressor – C2	Bitzer , 4PCS-10.2Y	1	50%/100% capacity control
Compressor – C3	Bitzer, 4J-13.2Y	1	
Compressor – C4	Bitzer, 4DC-5.2Y	1	
Condenser	GEA, MGC222H-09-EC3	1	No sub-cooling section
Condenser fan	Searle, 231–9091-EC 43	4	1.9 kW/fan, all fans VSD with some signal
Evaporator heat exchanger	Alfa Laval, AlfaChill 120	2	
Electronic expansion valve	Carel, E3V	2	
Heat exchanger	Ecolfex, GBS800H, 44 plates	1	

cooling capacity. Compressors C3 and C4 have only on/off controls, C2 has the capacity to offload two of its four cylinders (Bitzer Kühlmaschinenbau GmbH, 2014) and C1 is controlled via a variable speed drive (VSD) which operates from 20 Hz to 60 Hz (Searle Manufacturing Company, 2008). The four fans of the dry condenser (this condenser can be considered a cross-flow heat exchanger with multiple passes) are controlled by the same controller as the compressor bank and with only one control signal, therefore they were modelled as only one fan. These fans have two different maximum speeds depending on the time of the day, 53% of the plate value for day time operation and 100% for the night time operation. The CO_2 system, served by two evaporator heat exchangers together with two expansion valves, was considered the load of the refrigeration system. The CO_2 vessel is maintained at approximately 30 bar_g corresponding to a temperature of approximately –4.4 °C and serves the flooded evaporators installed in the display cabinets.

3. Software refrigeration model

The refrigeration system, displayed in Fig. 2, was modelled under steady state conditions with the five components as shown in this diagram using Matlab (MathWorks, 2011). For this the usual simplifying assumptions were used (for a list see, for instance, Arora, 2010). Other simplifications are mentioned as necessary. The R404A data from the software package CoolPack (Skovrup et al., 2012) were employed to help derive equations with fitted coefficients, i.e. Equations (6), (8), (12) and (16). The software model also took into consideration measurements of the installed system for the development of certain model parameters.

The *p–h* diagram in the right-hand panel in Fig. 2 indicates that the refrigeration cycle followed standard simplifying assumptions for a pure refrigerant. This meant that evaporation and superheating were modelled as isobaric processes with a constant pressure of 3.5 bar_g, which was also the suction set-point of the compressors in the installed system. The compression was thought of as an isentropic process with the implication that work input is a function of h_2 as the gradient of the entropy change decreases with an increasing degree of superheating (as indicated by the three entropy chain lines). The processes in the condenser and the sub-cooling were also modelled isobarically. The pressure range used here starts at 9 bar_g, which is approximately the minimum pressure of the installed system and extends to 18.5 bar_g corresponding to the maximum ambient temperature for which the installed system

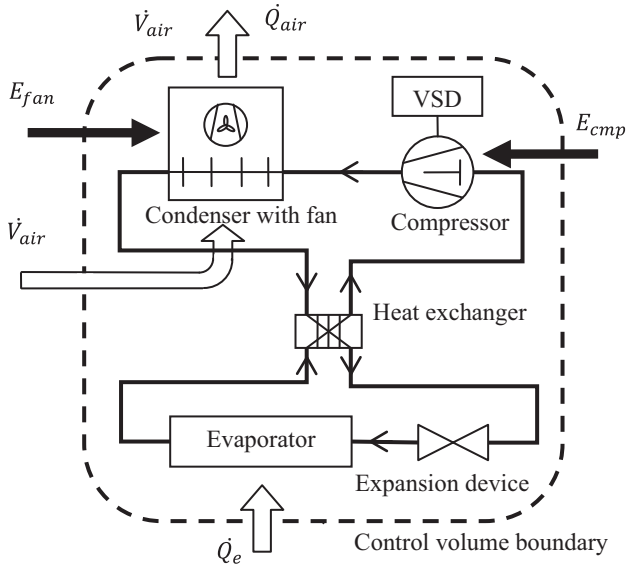

Schematics of refrigeration system

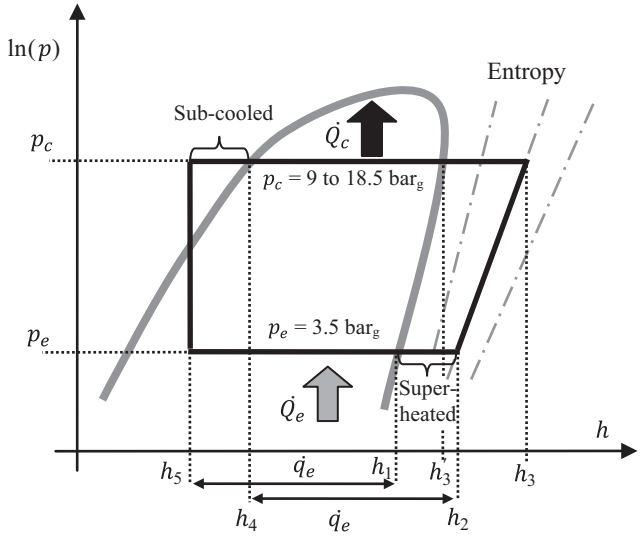

p-h diagram

Fig. 2 – Refrigeration system simulated by the software model and its *p–h* diagram.

Table 2 – Equations for refrigeration system components.

No	Component/Equation
Heat exchanger	
(3)	$\dot{q}_{HX} = \varepsilon \bar{c}_p \left(\vartheta_{l,sat} - \vartheta_{g,sat}\right)$
(4)	$\varepsilon = -5.52\times10^{-5}\frac{1}{\mathrm{kW}^2}\times\dot{Q}_e^2 + 1.68\times10^{-3}\frac{1}{\mathrm{kW}}\times\dot{Q}_e + 0.857$
(5)	$\bar{c}_p = 0.872\frac{\mathrm{kJ}}{\mathrm{kg\,K}}$
(6)	$\vartheta_{l,sat} = -0.0772\frac{^\circ\mathrm{C}}{\mathrm{bar}_g^2}p_c^2 + 4.69\frac{^\circ\mathrm{C}}{\mathrm{bar}_g}p_c - 19.14^\circ\mathrm{C}$
Compressor	
(7)	$h_3 = slope\times ln\left(\frac{p_{c,abs}}{3.5\ \mathrm{bar}_g + 1\ \mathrm{bar}}\right) + h_2$
(8)	$slope = 0.124h_2 - 24.8\frac{\mathrm{kJ}}{\mathrm{kg}}$
(9)	$E_{cmp} = 1.93\times E'_{cmp} + 3\ \mathrm{kW}$
(10)	$\dot{m}_{rf} = \frac{\dot{Q}_e}{h_2 - h_4}$
(11)	$E'_{cmp} = \dot{m}_{rf}\left(h_3 - h_2\right)$
(12)	$h_4 = -0.0814\frac{\mathrm{kJ}}{\mathrm{kg\,bar}^2}p_c^2 + 6.84\frac{\mathrm{kJ}}{\mathrm{kg\,bar}}p_c + 170\frac{\mathrm{kJ}}{\mathrm{kg}}$
Condenser	
(13)	$\dot{m}_{air,cdg} = \frac{\dot{Q}_{cdg}}{c_{air}\left(\vartheta_{l,sat} - 2\ \mathrm{K} - \vartheta_{on}\right)}$
(14)	$\dot{m}_{air,dsh} = \frac{\dot{Q}_{dsh}}{c_{air}\left(\bar{\vartheta}_2 - 2\ \mathrm{K} - \vartheta_{on}\right)}$
(15)	$\bar{\vartheta}_2 = \frac{\vartheta_{sh} + \vartheta_{l,sat}}{2}$
(16)	$\vartheta_{sh} = 4.90\times10^{-3}\frac{^\circ\mathrm{C}}{\mathrm{bar}^2}p_c^2 + 6.67\frac{^\circ\mathrm{C}}{\mathrm{bar}}p_c + 1.12\times10^{-4}\frac{^\circ\mathrm{C}}{(\mathrm{kJ/kg})^2}h_3^2 + 1.03\frac{^\circ\mathrm{C}}{\mathrm{kJ/kg}}h_3 - 0.0132\frac{^\circ\mathrm{C}}{\mathrm{bar\ kJ/kg}}p_c\times h_3 - 401^\circ\mathrm{C}$
Condenser fan	
(17)	$E_{fan} = 7.6\ \mathrm{kW}\ n_{fn\%}^3$
(18)	$n_{fn\%} = \begin{cases} 0, & p_c < 9.5\ \mathrm{bar}_g \\ \frac{n_{mx}}{1 + 0.25exp\left(-15\left(p_c\ \frac{1}{\mathrm{bar}_g} - 10\ \mathrm{bar}_g\right)\right)}, & 9.5\ \mathrm{bar}_g \le p_c \le 10.5\ \mathrm{bar}_g \\ n_{mx}, & p_c > 10.5\ \mathrm{bar}_g \end{cases}$

was designed (Searle Manufacturing Company, 2008). The p–h diagram also shows that the specific refrigeration load $\dot{q}_e$ not only equals the difference between h_1 and h_5, but also the difference between h_2 and h_4, because the heat exchanger in the left hand panel in Fig. 2 is thought of as having no heat losses, which eliminates the need to calculate the enthalpy h_5.

Table 2 lists all the equations used to describe the refrigeration cycle. This description started with the enthalpy of the saturated vapour at the outlet of the evaporator h_1 at p_e, which was found to be 363 kJ kg^{-1} (Skovrup et al., 2012). Equation (3), describing the superheating of the low pressure refrigerant to h_2, was based on the effectiveness-NTU method (Incropera and DeWitt, 1985). The relationship between ε and the cooling load $\dot{Q}_e$ shown in Equation (4) was based on measured data and has an r^2 of 0.864. As the changes of c_p in the area of interest were found to be small the average value was used as shown in Equation (5). Both temperatures in Equation (3) were determined by means of R404A data from the software CoolPack (–8.8 °C for $\vartheta_{g,sat}$).

The equations for the isentropic compression process, Equations (7) and (8), were derived based on the p–h R404A diagram in CoolPack. The measured data and the calculation based on an isentropic process show a good agreement ($r^2 = 0.957$ for a linear regression model). This gives support to modelling the compression process isentropicaly, although it is likely that the friction heat from the compressor and the heat rejected through the pipe work cancel each other out.

The mass flow rate, computed with Equation (10) where $\dot{Q}_e$ was used as the imposed cooling load, was used in Equation (11) to compute the theoretical power input into the compressor (without any losses, e.g., due to the electric motor). Next, this theoretical power was compared against the

measured consumption of the installed system to determine a simple regression model given in Equation (9).

As the cross flow, air cooled condenser of the refrigeration system has no subcooling section (GEA Searle, 2015) the condenser model was divided into only de-superheating and condensing sections. In the simplified approach chosen here the temperatures of the two condenser model sections (Ding, 2007) were either the saturated liquid temperature, $\vartheta_{l,sat}$ (in the condensing section), or the arithmetic mean $\bar{\vartheta}_2$ of $\vartheta_{l,sat}$ and the temperature of the superheated temperature after the compression process ϑ_{sh} (in the de-superheating section) as shown in Equation (15). Another option of modelling the condenser would have been to use an isothermal condenser approach based on the LMTD method without a de-superheating section as suggested by Stoecker and Jones (1983) and used in work by Yu and Chan (2008). However, Yu and Chan used an equation with empirical coefficients for the heat transfer coefficient, as for their model this coefficient was a function of airflow and the refrigeration mass flow. A further option would have been to model this cross flow condenser as a counter flow condenser as suggested by Xue et al. (2012). Both of these alternatives use their own simplifications and assumptions so that it was felt justifiable and adequate to use this simple condenser model for the purpose of this work.

Equations (13) and (14) calculated the air flow rate through the two condenser sections. $\dot{Q}_{cdg}\,(=\dot{m}_{rf}\,(h'_3-h_4))$ and $\dot{Q}_{dsh}\,(=\dot{m}_{rf}\,(h_3-h'_3))$ were the proportions of heat rejected in the condensing and de-superheating sections respectively. In these equations the 2 K constant acknowledges the requirement of a temperature gradient for heat flow to take place and is based on measurements on the installed system. The value of 1.006 kJ kg^{-1} K^{-1} was used as the specific heat capacity for air c_{air}.

Equation (17), which was based on the fan laws (ASHRAE, 2008), was used to calculate the power consumption of the condenser fans. The fan speed of the installed system was a function of the condenser pressure and its approximation is shown in Equation (18) (Searle Manufacturing Company, 2008). The maximum speed, n_{mx}, in this equation were 100% for the night time operation and 53% for the day time operation. As discussed in Section 1.1, the influence of the power use of the condenser fans on the COSP is significant and therefore will be investigated within the Matlab program described next.

3.1. *Matlab program*

The main program had three loops as illustrated in Fig. 3. The two outer loops were for the independent variables $\dot{Q}_e$ and ϑ_{on} for which the energy consumption $E_{tot}\,(=E_{cmp}+E_{fan})$ was calculated. Their values were passed on to the program in two vectors: $\vec{\dot{Q}}_e$ for the useful refrigeration effect as the load of the system and $\vec{\vartheta}_{on}$ for the ambient temperature, which was the temperature of the air entering the condenser. For the installed system night time and day time operation modes were also evaluated separately.

The flowcharts in Fig. 4 and Fig. 5 display the Matlab functions called by the main program shown in Fig. 3 to calculate the fan speed. Fig. 4 is based on the control algorithm of the installed system implementing Equation (18) with the distinction of three control modes according to p_c (also referred to as

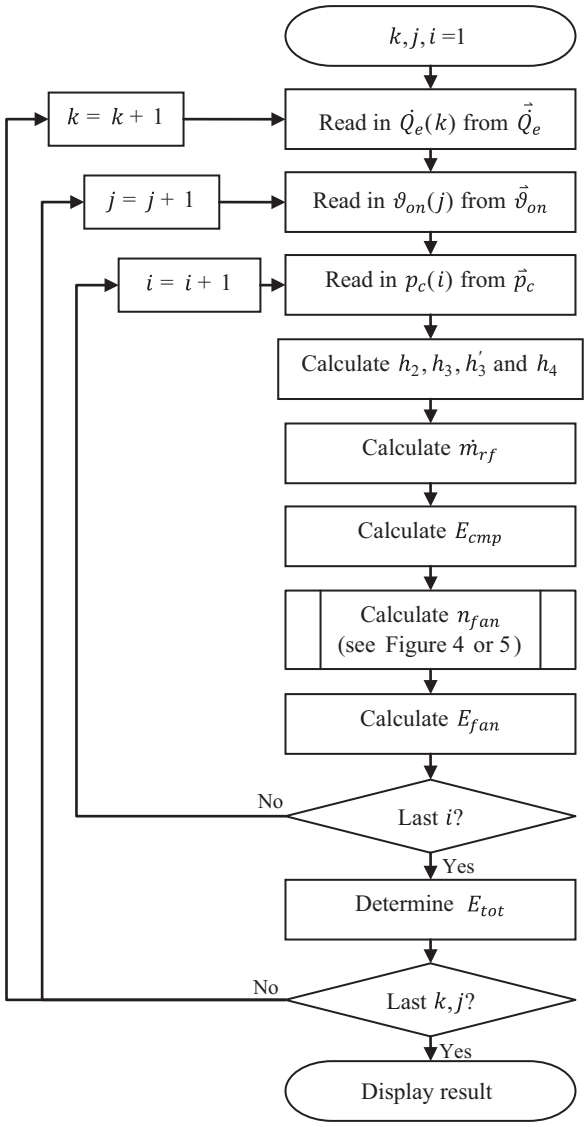

Fig. 3 – Matlab model flowchart of main program.

"old control" below). If the pressure was below 9.5 bar$_g$ a heat rejection due to convection of 15 kW was assumed based on the study of the installed system. Fig. 5 does not require the day/night mode differentiation as this control uses a different approach.

The main purpose of the third loop was to determine whether the air flow through the condenser was able to remove the rejected heat from the condenser at a given condenser pressure. Beginning with the minimum value for p_c this loop calculated all the required enthalpies and the refrigerant mass flow rate $\dot{m}_{rf}$ and then called a separate function to calculate the fan speed (either the old control Matlab function shown in Fig. 4 or the COSP maximising Matlab function displayed in Fig. 5). This function returned an error if the maximum air flow rate was insufficient causing the main program to record a high value (i.e. 9e99) in the vector storing all values for the fan power. If no error was returned the program calculated the fan power consumption E_{fan}. Once the third loop had calculated all the possible combinations, the lowest possible compressor power

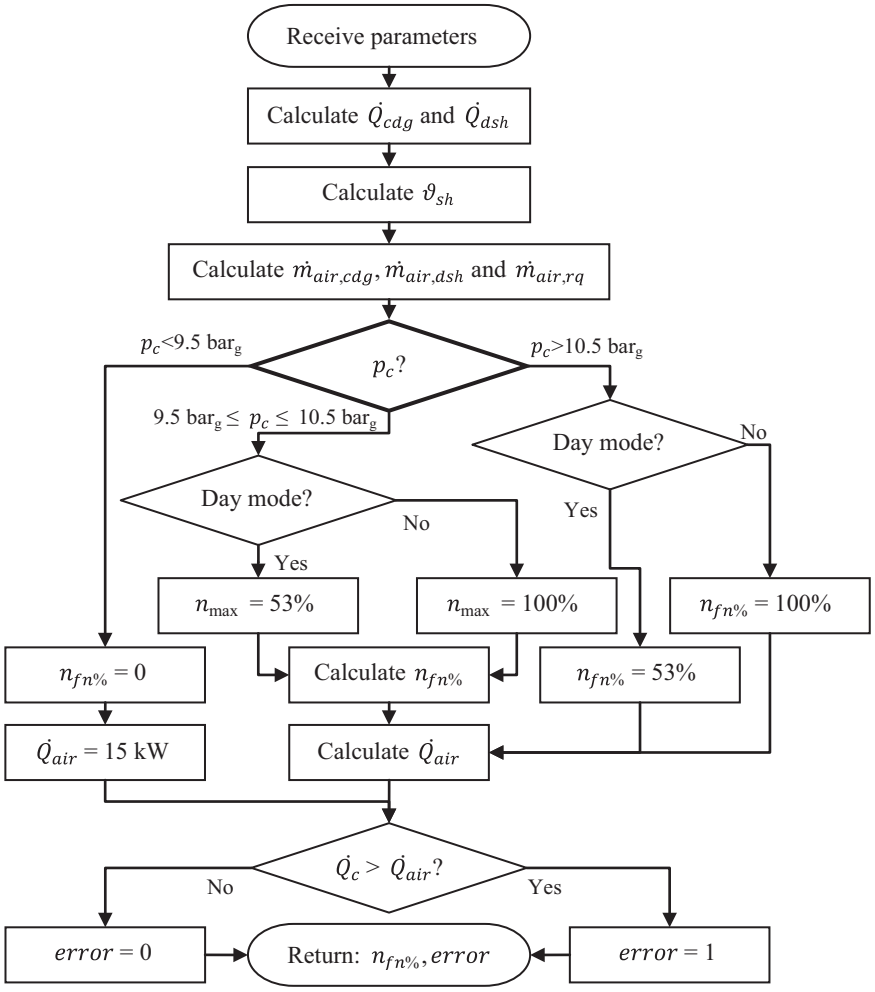

Fig. 4 – Matlab function flowchart to calculate the condenser fan speed according to the settings in the installed system.

and lowest total power together with their respective fan power values were stored in vectors for display after all values in $\vec{Q}_e$ and $\vec{\vartheta}_{on}$ had been processed.

3.2. *Error estimation*

To test the accuracy of the model consumption and temperature data averaged for 15 minute intervals from the installed system from 1 June 2014 to 30 November 2014 were compared with predictions for the model including fans. Fig. 6, which displays the values normalised to the maximum measured power, shows that the majority of data points (88.5%) lie within the ±10% boundaries. From approximately 75% of the measured consumption onwards the model tends to overestimate the consumption. From approximately 28% to about 45% the model overestimates the consumption for a number of data points, which may be due to the way the fan control has been simulated.

The root mean square error was also calculated for all the data points and found to be 1.43 kW or 8.22% of the average measured consumption. The mean bias error is 0.480 kW indicating that for the data set used the model tends to overpredict the energy consumption.

4. Results

The consumption of the refrigeration model was calculated for the *COSP* maximising method (see Fig. 5), and for the day time and night time operation modes according to the old method as described in Fig. 4. The results for the cooling load of 20 kW are displayed in the left hand panel of Fig. 7. This graph contains lines for the total power use (solid lines) and the compressor power (dotted lines or with markers). The total power for the *COSP* maximising control method is below the old methods for the outside temperature to approximately 15 °C when all three lines converge. From approximately 16.5 °C onwards the graphs for the total power consumption spread out whilst the different compressor consumption lines remain close together. In this temperature range the compressor in the night time mode consumes the least power, closely followed by the day time mode. The blue line with markers for the *COSP* maximising control indicates that the compressor input power is somewhat higher. When examining the total power consumption the results are reversed. The *COSP* maximising approach is predicted to have an appreciably lower total power use than both the day time and night time

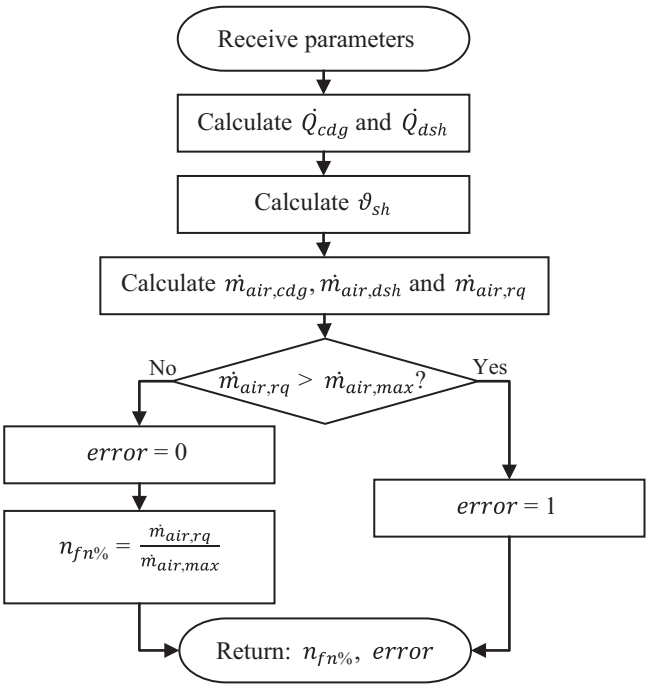

Fig. 5 – Matlab function flowchart for the condenser fan speed to maximise *COSP*.

operations. For instance at 19 °C the total consumption of the system in night time mode is 16 kW, of which 7.6 kW, or 47.5%, is the condenser fan power. The day time mode uses about 9.6 kW and the new approach only 8.8 kW. In other words the lower compressor power (and therefore the higher *COP*) requires a higher total power input.

The results for a $\dot{Q}_e$ of 20 kW, 50 kW and 80 kW are displayed in the right hand panel of Fig. 7. This graph shows that the point where the lines of all three approaches touch each other moves towards the lower temperature range as the cooling load increases. Below this point, the gap between the *COSP* maximising approach and the old approaches increases with increasing cooling load. For the temperature range beyond this point the gap narrows and disappears almost completely for the day time operation and the *COSP* maximising approach at the highest refrigeration load. This is due to the higher requirements for the air flow rate, $\dot{V}_{air}$, for the higher load as more heat needs to be removed from the condenser.

Fig. 8 compares the *COSP* maximising approach with the one used in the installed system based on the data collection period from 1 June 2014 to 30 November 2014. It shows that the *COSP* maximised system used approximately 583 kWh/month or 4.5% less energy.

5. Discussion and conclusions

The main insights gained from the simple equation relating the *COSP* to the *COP* are supported by results from the software model based on an R404A supermarket refrigeration system. This insight included appreciating the influence the cooling load has on the performance gap between a *COP* and a *COSP* optimised system. The two graphs based on Equation (2) in Fig. 1 show that for the 100% cooling load the difference between these two systems is considerably smaller than for the 20% case. A similar trend can be observed in the right hand diagram of Fig. 7 which indicates that, for the temperature range after the point where all three lines touch each other, the performance gap between the old control methods and the

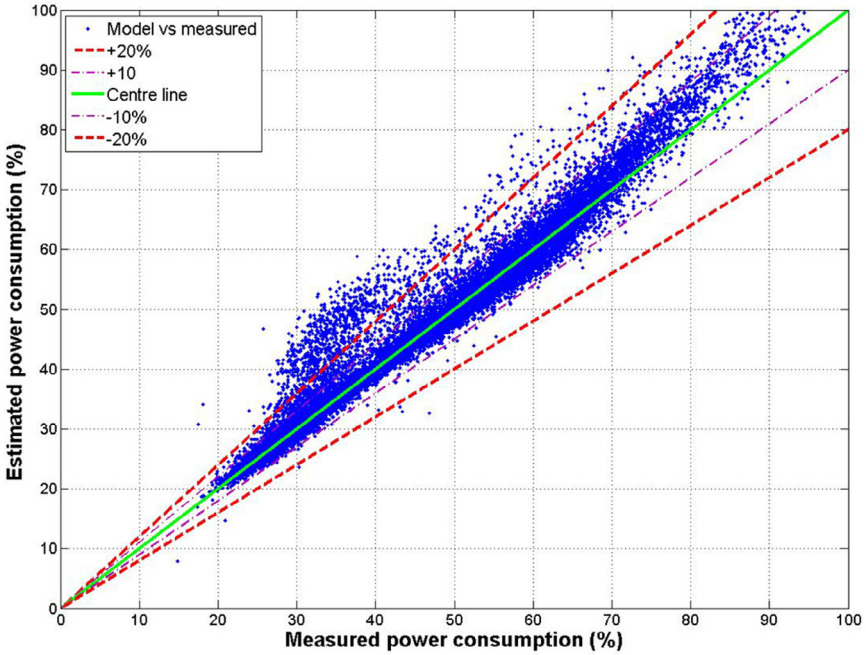

Fig. 6 – Scatter plot of the estimation from the complete model vs the measured data from the installed refrigeration system.

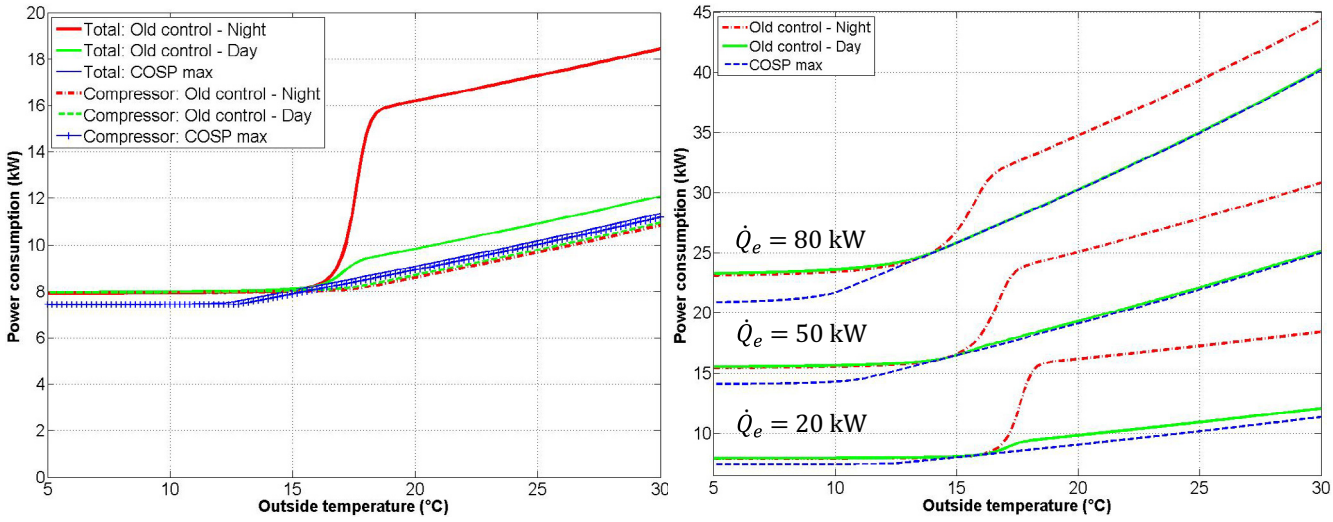

a) Cooling load = 20 kW b) Total power consumption

Fig. 7 – Comparing different fan control methods for different cooling loads. (For interpretation of the references to colour in this figure legend, the reader is referred to the web version of this article.)

COSP maximising approach narrows with rising $\dot{Q}_e$. A further point of interest is the influence of the condenser fan power use on the efficiency figures for lower cooling loads. The left hand panel in Fig. 1 shows that under part-load conditions this is more significant than with a full-load and the left hand graph in Fig. 7 suggests that it may be up to approximately half the overall power consumption. This conclusion is in line with the results for dry air chillers reported by Yu and Chan who also concluded that that overall energy consumption depends not only on the outdoor temperature, but also on the cooling load (Yu and Chan, 2005; Yu et al., 2006; Yu and Chan, 2008).

The significance of this insight is that for optimal overall control algorithms not only does the design point need to be considered, but part load conditions also do, because a refrigeration system arguably operates most of the time away from its design point. Otherwise the misconception that the "fan power is only a small fraction of the total power consumption" (Ge and Tassou, 2000) may influence the approaches to controlling condenser fans and compressors. Such a control method should strive to closely match the fan speed to the rejected heat. This can have a significant impact on the overall power use because (a) the installed system showed that the maximum fan power is comparable to the two smaller compressors of the installed system and (b) the power consumption rises by the power of 3 for the fan speed.

The work above showed that it is possible to improve the *COSP* by driving the compressor somewhat harder, and therefore reducing the *COP* of the core refrigeration system to allow the condenser fan to reduce its speed. This approach was implemented in the Matlab model with an estimated energy reduction of 4.5% for the six month data set. Hence, this idea should be taken forward to verify that the energy saving potential can also be achieved in practice. To do this the system may have to be modified to allow the measurement of the mass flow rate to calculate the cooling load. In addition, the control algorithm has to be modified to allow the computation of the fan speed according to the heat rejection requirements.

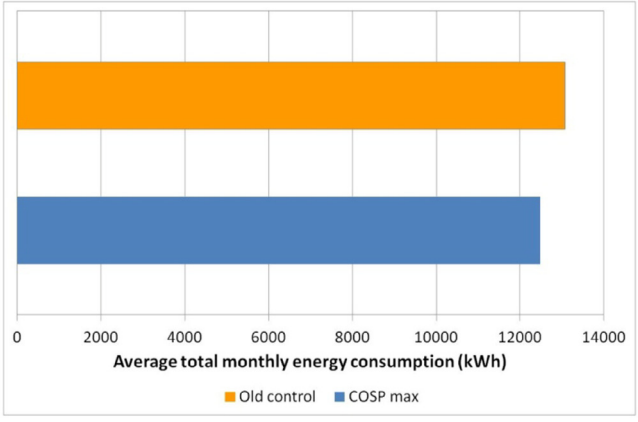

Fig. 8 – Bar graph of energy consumption for old and COSP maximising control approach.

Acknowledgements

This research was partly funded by the EPSRC grant (Grant Ref EP/G037477/1) through the E-Futures Doctoral Training Centre. The authors would also like to gratefully acknowledge the support of Marks & Spencer and Retail Solutions UK, part of Emerson Climate Technologies, retail solutions, in particular Mr Keith Bertie and Mr Matthew Maeer.

REFERENCES

Arora, R.C., 2010. Refrigeration and Air conditioning. PHI Learning, New Delhi.

ASHRAE., 1997. 1997 ASHRAE Handbook Fundamentals. ASHRAE, Atlanta.
ASHRAE., 2002. 2002 ASHRAE Handbook, Refrigeration. ASHRAE, Atlanta.
ASHRAE., 2008. 2008 ASHRAE Handbook, Heating, Ventilating, and Air-Conditioning Systems and Equipment. ASHRAE, Atlanta.
Bitzer Kühlmaschinenbau GmbH., 2014. Competence In Capacity Control. Bitzer Kühlmaschinenbau, Sindelfingen, Germany.
Braun, M.R., Beck, S.B.M., Altan, H. 2014. Comparing COP optimization with maximizing the coefficient of system performance for refrigeration systems in supermarkets. 15th International Refrigeration and Air Conditioning Conference. Purdue: Purdue University.
BS EN 13771-1., 2003. Compressor and Condensing Units for Refrigeration – Performance Testing and Test Methods – Part 1: Refrigeration Compressors. BSI, London.
BS EN 13771-2., 2007. Compressors and Condensing Units for Refrigeration – Performance Testing and Test Methods – Part 2: Condensing Units. BSI, London.
Çengel, Y.A., Boles, M.A., 2007. Thermodynamics: An Engineering Approach. McGraw-Hill Higher Education, Boston.
da Cunha, I. (2010) Refrigeration Systems, Energy Efficiency Reference Guide. Montréal: CEATI International.
Ding, G.-L., 2007. Recent developments in simulation techniques for vapour-compression refrigeration systems. Int. J. Refrig. 30, 1119–1133.
Ge, Y.T., Tassou, S.A., 2000. Mathematical modelling of supermarket refrigeration systems for design, energy prediction and control. P. I. Mech. Eng. A. J. Pow. 214, 101–114.
GEA Searle, 2015. Specification – MGC222H-EC855. GEA Searle, Fareham, UK.
Incropera, F.P., DeWitt, D.P., 1985. Introduction to Heat Transfer. John Wiley & Sons, New York.
Manske, K.A., Reindl, D.T., Klein, S.A., 2001. Evaporative condenser control in industrial refrigeration systems. Int. J. Refrig. 24, 676–691.
MathWorks., 2011. MATLAB 7, Getting Started Guide. The MathWorks, Natick.
Pearson, A., 2008. Specifying and selecting refrigeration and freezer plant. In: Evans, J.A. (Ed.), Frozen Food Science and Technology. Blackwell Publishing Ltd, Oxford.
Searle Manufacturing Company., 2008. CCU-CO2-100, Walk in Condensing Unit for CO2 Cascade System. Searle Manufacturing Company, Fareham.
Skovrup, M.J., Jakobsen, A., Rasmussen, B.D., Andersen, S.E. 2012. *CoolPack* (Version: 1.5). http://en.ipu.dk/Indhold/refrigeration-and-energy-technology/coolpack.aspx (accessed 02.09.14).
Stoecker, W.F., Jones, J.W., 1983. Refrigeration and Air Conditioning. McGraw-Hill Higher Education, New York.
Xue, X., Feng, X., Wang, J., Liu, F., 2012. Modeling and simulation of an air-cooling condenser under transient conditions. Procedia Eng. 31, 817–822.
Yu, F., Chan, K., 2005. Optimum condenser fan staging for air-cooled chillers. Appl. Therm. Eng. 25, 2204–2218.
Yu, F., Chan, K., Chu, H. 2006. Efficiency improvements of air-cooled chillers equipped with high static condenser fans. International Refrigeration and Air Conditioning Conference. West Lafayette, US: Purdue University.
Yu, F.W., Chan, K.T., 2008. Optimizing condenser fan control for air-cooled centrifugal chillers. Int. J. Therm. Sci. 47, 942–953.
Yuventi, J., Mehdizadeh, R., 2013. A critical analysis of Power Usage Effectiveness and its use in communicating data center energy consumption. Energy Build. 64, 90–94.